

# Numerical investigation of natural convection in a cavity using an open geometry

Boris Brangeon<sup>1,\*</sup>, Alain Bastide<sup>1</sup>, Patrice Joubert<sup>2</sup> and Michel Pons<sup>3</sup>

<sup>1</sup>PIMENT, Université de La Réunion, 117 Avenue du Général Ailleret 97430 Le Tampon, France.

<sup>2</sup>LEPTIAB, Université de La Rochelle, Avenue M. Crépeau, 17042 La Rochelle Cedex 1, France.

<sup>3</sup>LIMSI CNRS UPR3251, BP 133, 91403 Orsay Cedex, France.

\*Corresponding email: [boris.brangeon@univ-reunion.fr](mailto:boris.brangeon@univ-reunion.fr)

## SUMMARY

This paper presents a numerical investigation of airflow in an open geometry. The case under consideration is a room with two opposite and decentred openings which create a strong potential for ventilation. The building's characteristic dimensions are the following:  $H=2.50$  m height and  $W=6.50$  m width. A temperature difference between the walls and the outside air is fixed, resulting in a characteristic Rayleigh number ( $Ra$ ) ranging from  $10^5$  to  $10^7$ . This room model proceeds from a benchmark exercise "ADNBATI" (<http://adnbati.limsi.fr>) coordinated by the "Centre National de la Recherche Française -CNRS-".

## IMPLICATIONS

This paper presents and discusses the results of this numerical study. Velocity, temperature fields, as well as heat transfer at the walls are analyzed. Values of the Nusselt number and of the mass flow rate according to the Rayleigh number are established from these first results.

## KEYWORDS

*Direct Numerical Simulation, Natural convection, Open enclosures, Boundary conditions.*

## INTRODUCTION

For night cooling of buildings, two choices are possible: mechanical ventilation and/or natural ventilation. The later mechanism is an efficient passive cooling process for moderate hot climates and is investigated in this paper to remove excessive heat accumulated during the day. In the present study, investigations are performed to simulate natural convection within a building model. The geometrical configuration is an open room with two opposite and decentred openings to create a strong potential for natural ventilation. The room model proceeds from a benchmark exercise "ADNBATI" (Stephan, 2010) coordinated by the "Centre National de la Recherche Française -CNRS-". This study is the first step in a global work (wall to fluid heat transfer, flow zones definition, turbulence model test and selection, radiative heat transfer, etc...), but here only natural convection is considered. The building characteristics dimensions are the followings:  $H=2.50$  m height and  $W=6.50$  m width (see Figure 1). The opening ratio  $H_1/H_2$  equals 0.5.  $Ra$  is the Rayleigh number based on the cavity height  $H$ . A temperature difference between the inside walls and the outside air is fixed, resulting in a characteristic Rayleigh number ranging from  $10^5$  to  $10^7$ .

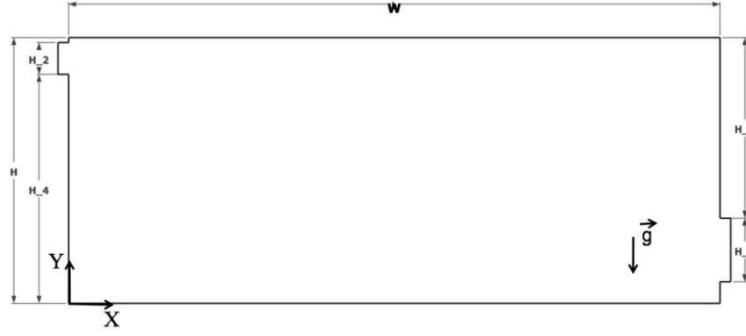


Figure 1. Cavity problem.

Table 1. Geometry characteristic parameters.

	Value [m]
Height low East opening $H_1$	0.6
Height low West opening $H_2$	0.3
Height wall East $H_3$	1.7
Height wall West $H_4$	2.15

## METHODS

### Governing equations

We consider a cavity of height  $H$  and width  $W$  traversed by an incompressible Newtonian viscous fluid of kinematic viscosity  $\nu$  and thermal diffusivity  $\kappa$  (see figure 1). The fluid density  $\rho$  is assumed to depend only on temperature :  $\rho = \rho_0[1 - \beta(T - T_0)]$ , where  $\beta$  is the thermal expansion coefficient. The usual dimensionless Boussinesq 2D Navier-Stokes equations are then:

$$\frac{\partial u}{\partial x} + \frac{\partial v}{\partial y} = 0 \quad (1)$$

$$\frac{\partial u}{\partial t} + u \frac{\partial u}{\partial x} + v \frac{\partial u}{\partial y} = -\frac{\partial P_m}{\partial x} + PrRa^{-1/2}\nabla^2 u \quad (2)$$

$$\frac{\partial v}{\partial t} + u \frac{\partial v}{\partial x} + v \frac{\partial v}{\partial y} = -\frac{\partial P_m}{\partial y} + PrRa^{-1/2}\nabla^2 v + Pr\theta \quad (3)$$

$$\frac{\partial \theta}{\partial t} + u \frac{\partial \theta}{\partial x} + v \frac{\partial \theta}{\partial y} = Ra^{-1/2}\nabla^2 \theta \quad (4)$$

The corresponding equations are made dimensionless by introducing  $H$ ,  $U_{CN} = \kappa Ra^{1/2}/H$  (Bejan, 1984) and  $\Delta T$  as reference quantities for length, velocity and temperature difference. The Prandtl number  $Pr$  is fixed to 0.71.

### Boundary conditions

The wall's temperature is set to a constant temperature,  $T_w$ , higher than the outside temperature except for the frames of the openings for which an adiabatic condition is applied (see figure 1). A non-slip boundary condition is imposed on the velocity along all the walls.

Low East opening/ high West opening: the openings are framed, in order to take the thickness of the walls into account. The imposed conditions at the end of these frames ( $X = -0.1$  m and  $X = 6.6$  m) are the followings: if  $\vec{V} \cdot \vec{n} < 0$  then  $\theta = 0$ , else  $\frac{\partial \theta}{\partial x} = 0$ .

The choice of the boundary conditions that must be applied to the velocity and the pressure is delicate for open geometries with natural convection flow. Indeed, the resulting thermosiphon

flow is the result of the balance between the forces due to buoyancy and the head losses between the low East and the high West openings of the cavity. However, no choice appears to be trivial to impose velocity or pressure conditions at the low East opening. We here propose the use of a boundary condition from a Stokes' phenomenon to the openings. We consider that at the low East opening, the following hypotheses are respected: the flow is steady and incompressible, the viscous terms are negligible and the rotational of the velocity equals zero. We can therefore relate the mass flow rate to the difference of pressure between the low East and the high West opening by the relation:

$$\int_{H_2} (p + \rho g z) \cdot dA - \int_{H_1} (p + \rho g z) \cdot dA = \int_{H_1} \frac{1}{2} \rho |V|^2 \cdot dA \quad (5)$$

This boundary condition is identical to the one which was proposed during a set benchmark in the framework of the network AMETH (Desrayaud, 2007) constituted of an asymmetrically-heated vertical channel, treated experimentally by Webb and Hill (Webb and Hill, 1989). The comparison of the two numerical simulations between different French research teams and our personal works, turns out to be conclusive for  $Ra$  equals to  $5 \cdot 10^5$ . The benchmark ADNBTI (Stephan, 2010) examines this issue and is currently subjected to a confrontation between numerical research codes and commercial codes. In our simulation, the boundary conditions are the following:

- at the low East opening: if  $\vec{V} \cdot \vec{n} < 0$  then  $P_m = -\frac{1}{2S_e^2} G^2$  where  $\vec{n}$  is exterior normal vector,  $G$  is mass flow rate and  $S_e$  is low East opening section. Locally, if  $\vec{V} \cdot \vec{n} > 0$  then  $P_m = -\frac{1}{2} |V|^2$ , else  $P_m = 0$ .
- at the high West opening: a free-jet condition is imposed:  $P_m = 0$ .

### Numerical approach: spatial and temporal discretization

The numerical code has been developed thanks to the environment OpenFOAM (OpenFOAM, 2010). The time derivatives in the momentum and in the energy equations are performed by a second-order backward differentiation. The convection terms are approximate using a second-order Adams-Bashford extrapolation method. The diffusion terms are implicitly treated. The resulting Helmholtz systems are solved by a direct solver. Finally, the general numerical scheme is the following:

$$\frac{3f^{n+1} - 4f^n + f^{n-1}}{2\Delta t} + 2 \left( \frac{\partial f u_j}{\partial x_j} \right)^n + \left( \frac{\partial f u_j}{\partial x_j} \right)^{n-1} = \left( \frac{\partial}{\partial x_j} \frac{\partial f}{\partial x_j} \right)^{n+1} \quad (6)$$

Pressure-velocity coupling is obtained by an incremental rotational projection method.

In the present study, a collocated finite volume method has been used. The case has been computed with a  $1024 \times 825$  grid size. The local Reynolds number ( $Re$ ) obtained is lower than 20 and the non-dimensional wall distance in terms of wall units ( $y^+$ ) is less than 1. These quantities are displayed here for information on the quality of the mesh and will be submitted to an accurate study for more severe flows conditions for which turbulence models will be used. The dimensionless time step ( $\Delta t$ ) varies from  $1.25 \cdot 10^{-4}$  ( $Ra = 10^5$ ) to  $0.85 \cdot 10^{-4}$  ( $Ra = 10^7$ ).

## RESULTS AND DISCUSSIONS

At least 60 dimensionless time units are used for this statistics calculation, in order to obtain the statistical values of  $u$ ,  $v$  and  $\theta$ . A steady laminar flow is obtained for  $Ra=10^5$  and unsteady for  $Ra=10^6$  and  $Ra=10^7$ .

Figure 2 displays the isotherms and streamlines fields for three values of the Rayleigh numbers:  $Ra=10^5$ ,  $10^6$  and  $10^7$ . In the three cases, the flow which goes from the low East opening to the high West opening splits into two main flows. The main one is a cold jet, crawling on the floor surface until the West wall along which he finally goes up. The second moderate flow, goes right up along the East wall and joins the high West opening staying stuck to the ceiling. Between these two flows, two contrarotative cells exist, which progressively lengthen horizontally while  $Ra$  increases. The first one is localized above the jet, in the main part of the cavity ( $c_{1,10^5}(x = 1.11; y = 0.47)$ ,  $c_{1,10^6}(x = 0.70; y = 0.36)$ ,  $c_{1,10^7}(x = 0.52; y = 0.40)$ ). The second one is located between the first cell and the heated surface of the ceiling ( $c_{2,10^5}(x = 0.46; y = 0.70)$ ,  $c_{2,10^6}(x = 0.71; y = 0.70)$ ). It becomes more and more intense. A third cell along the East wall which progressively disappears while  $Ra$  increases.

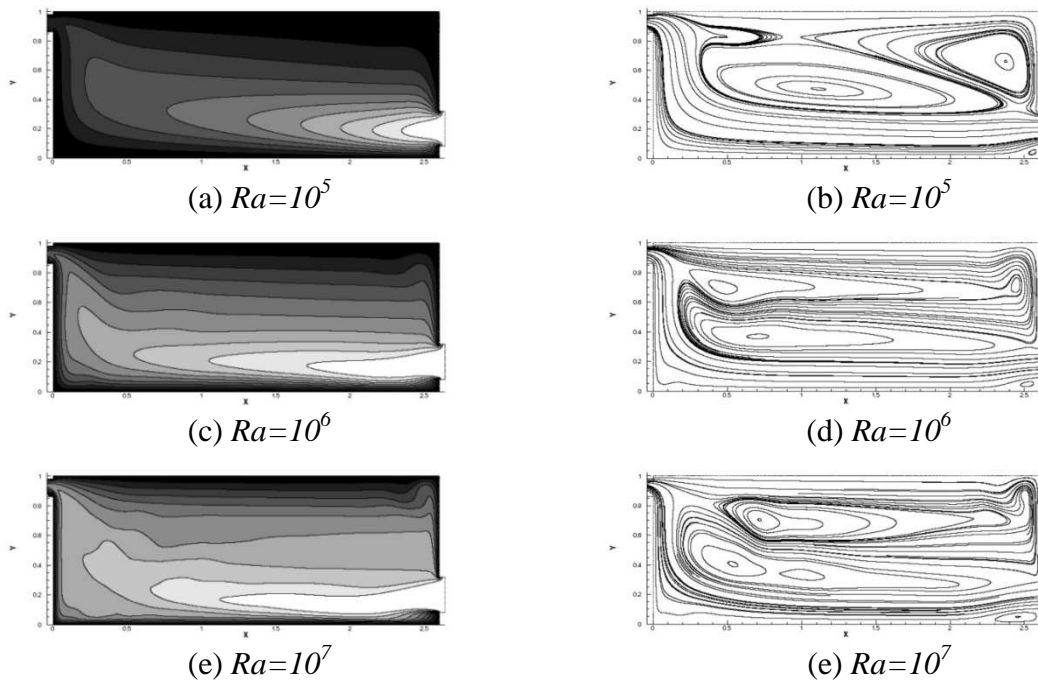


Figure 2. Average solutions. Left: average temperature field. Right: streamlines of average flow.

In addition, a penetration of fresh air becomes apparent and turns out to be stronger in the room as the Rayleigh number increases, that is to say when the convection acquires more importance compared to diffusion. The thickness of the boundary thermal layers decreases and the heart of the cavity cools down.

The third figure shows the evolution of the horizontal and vertical components of the velocity vector (respectively  $u$  and  $v$ ) at the East opening (see figures 3(a) and 3(b)) and to the West opening (see figures 3(c) and 3(d)). The general velocity profiles at the East opening tends to distort itself and decreases rapidly when the temperature difference between the incoming air and the walls increases (see figure 3(a)). This may be explained by a vertical, Rayleigh-Benard type flow in the low part of the room, as these instabilities tend to contradict the inlet jet. At the West opening, the fluid re-enters the cavity within a height which can reach a

quarter of the outlet section for  $Ra= 10^6-10^7$ . This phenomenon does not exist for the lower Rayleigh number.

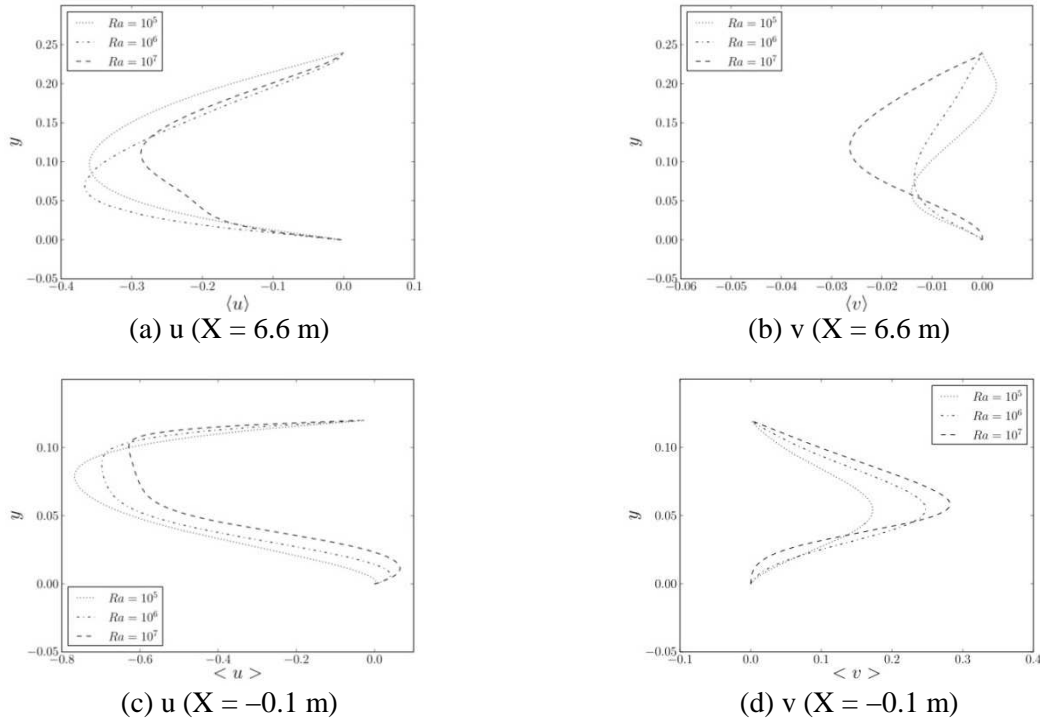


Figure 3. Average horizontal (left) and vertical (right) velocity profiles at inlet: 3(a) et 3(b) and outlet: 3(c) et 3(d).

The average values of the numbers of Nusselt  $Nu$ , obtained along the hot vertical and horizontal walls ( $Nu_i = \frac{1}{H_i} \int \frac{\partial \theta}{\partial x} dn$ ), are reported in table 2(a) ( $Nu_F$  for the floor,  $Nu_R$  for the ceiling,  $Nu_O$  for the Western wall and  $Nu_E$  for the Eastern wall). The results indicate that the heat transfers are lower along the ceiling. For  $Ra= 10^5$ , the convective exchange on the vertical Western wall is lower than the one on the Eastern wall, even though the exchanges are balanced when  $Ra$  has superior values. It may be explained by the fact that for this value, the horizontal jet is weak and cannot drag the cold fluid up to the West wall. The average temperature of the fluid which is coming out from the high opening gives an indication on the quantity of total heat carried away outside by the fluid.

Quantitatively, we observe that the mass flow rate  $D_v$  remains low. It will be interesting to study if efficient rate of air exchange for the night cooling may be obtained when the number of Rayleigh has more important values.

Table 2. Average Nusselt number (a) and summary of average flow results (b).

$Ra$	$10^5$	$10^6$	$10^7$	$Ra$	$10^5$	$10^6$	$10^7$
$Nu_F$	3.60	8.01	17.95	$G$	0.023	0.021	0.018
$Nu_R$	0.80	1.49	2.97	$D_v$	0.223	0.654	1.775
$Nu_O$	1.58	7.21	17.41	$\tau$	0.085	0.251	0.600
$Nu_E$	3.41	7.49	17.60	$\theta_m$	0.850	0.700	0.550

(a)

(b)

## CONCLUSION

A direct numerical simulation of the natural airflow in an open cavity has been presented and discussed. We choose a room model which will be used as a basis for other simulations in

order to expand our knowledge in regards to night cooling. The validation of the choice concerning the boundary condition on the inlet pressure has been realized on the basis of a comparison with the numerical data of the benchmark for  $Ra = 5.10^5$  (Desrayaud, 2007). The first results that we are presenting in the benchmark configuration here ADNBTATI (Stephan, 2010) will be confronted in a near future to other team's results especially concerning the values of the numbers of Nusselt and the obtained mass flow rate. The future perspectives would be, for example, to establish the evolution of the number of Rayleigh ( $Nu = \alpha Ra^\gamma$ ). In order to realize a more realistic situation,  $Ra = 10^8-10^{10}$ , it would be indispensable to take turbulent models so as to obtain a time step compatible with parametrical simulations. A numerical approach of the flows through the large eddy simulation will be used for the superior numbers of Rayleigh to be found in the building.

## ACKNOWLEDGEMENT

This work has been supported by French Research National Agency (ANR) through "Habitat intelligent et solaire photovoltaïque" program (project 4C n°ANR-08-HABISOL-019) and project "ADNBATTI", financed by the Energy program of CNRS (PE09-3-2-1-1).

## REFERENCES

- Bejan A. Convection heat transfer. John Wiley and Sons, 1984.
- Desrayaud G., Bennacer R., Caltagirone J.P., Chenier E., Joulin A., Laaroussi N. and K.Mojtabi, Etude numérique comparative des écoulements thermoconvectifs dans un canal vertical chauffé asymétriquement. In VIIIème Colloque Interuniv. Franco-Québécois, Mai 2007, 6 pages.
- Stephan L., Wurtz E., Bastide A., Brangeon B., Jay A., Goffaux C. and Pons C., Benchmark de ventilation naturelle traversante (ADNBATTI). Actes Int. Building Performance Simulation Association (IBPSA-France) Conf., 9-10 Novembre 2010, Moret-sur-Loing, France, Ed. J. J. Roux & G. Krauss, Article 'PONS r98.doc', 2010.
- Webb B.W and Hill D.P., High Rayleigh number laminar natural convection in an asymmetrically heated vertical channel. Journal Heat Transfer, (111), 1989, 649–656.
- OpenFOAM 1.7, <http://www.openfoam.com>, 2010.

Nomenclature					
$C_{cell,Ra}$	convective cell center	[-]	$U_{CN}$	reference velocity	[-]
$D_v$	mass flow rate	[m <sup>2</sup> .h <sup>-1</sup> ]	$x, y$	dimensionless spatial coordinate	[-]
$G$	dimensionless mass flow rate	[-]	$Pr$	Prandtl number	[-]
$g$	gravitational acceleration	[m.s <sup>-2</sup> ]	Greek symbols		
$H$	cavity height	[m]	$\beta$	thermal expansion	[K <sup>-1</sup> ]
$H_1, H_2$	height inlet and outlet	[m]	$\kappa$	thermal diffusivity	[m <sup>2</sup> .s <sup>-1</sup> ]
$H_3, H_4$	height wall East and West	[m]	$\nu$	kinematic viscosity	[m <sup>2</sup> .s <sup>-1</sup> ]
$P_m$	dimensionless dynamic pressure	[-]	$\rho$	fluid density	[kg.m <sup>-3</sup> ]
$Ra$	Rayleigh number	[-]	$\theta$	dimensionless temperature	[-]
$t$	dimensionless time	[-]	$\theta_m$	dimensionless averaged temperature	[-]
$T$	temperature	[K]			
$\Delta T$	temperature difference	[K]			
$u, v$	dimensionless velocity components	[-]			